

Large-Scale Resonant Modification of the Polar Ionosphere by Electromagnetic Waves

A. Y. Wong, P. Y. Cheung, M. J. McCarrick, J. Stanley, R. F. Wuerker, R. Close, and B. S. Bauer
Department of Physics, University of California, Los Angeles, California 90024-1547

E. Fremouw

Northwest Research Associates, Inc., Bellevue, Washington 98005

W. Krueer and B. Langdon

Lawrence Livermore National Laboratory, University of California, Livermore, California 94550

(Received 11 October 1988)

Large-scale density modification was optimally achieved by electromagnetic waves whose frequency matched the plasma frequency at a height where the ionospheric density profile was flat. The density in this region was dramatically clamped during the morning when it normally increases from solar ionization. Electromagnetic wave propagation in the polar magnetic field geometry and strongly resonantly enhanced electrostatic fields over a large region of constant density account for the observation.

PACS numbers: 94.20.-y, 52.25.Sw, 52.70.Gw

We report the observation of large-scale modification of the polar ionosphere by electromagnetic (EM) waves at modest power density ($0.1 < p_0 < 1 \text{ mW/m}^2$). Maximum density perturbations are observed when the excitation frequency matches the plasma frequency of the location in the density profile where the gradient is nearly zero. This observed sensitive dependence on the ionospheric density and its gradient indicates that the plasma resonance and the enhancement of the incident field control the dynamic modification process. The nearly vertical polar magnetic field geometry and the vertical density profile made it possible for a large cone of EM rays to reach the resonant height to create the large-scale perturbation. The long energy confinement time ($\cong 10^3$ sec, as determined mainly by the recombination process¹) allows the incident energy absorbed by the ionosphere to be accumulated and a large region to be affected in the course of time. A consequence of the present experiment is the controlled coupling to large scale natural phenomena.

The observation reported here is significantly different from previous experiments² in the location and extent of the perturbation at resonance, the magnetic field geometry, the deliberate choice of matching conditions with and without solar uv ionization, and the diagnostics.

The experiments were performed at the newly completed HIPAS Observatory, located near Fairbanks, AK (geographic coordinates: latitude $64^\circ 52' 22''$ N, longitude $146^\circ 50' 06''$ W). The antenna was radiating EM waves vertically upward with *O*-mode polarization (*E* vector rotating in a direction counter to the electron cyclotron gyration). This mode was chosen to avoid strong absorption in the lower ionosphere and to produce a highly enhanced oscillating electric field component along the vertical density gradient which is nearly parallel to the magnetic field. The frequency is 3.349 MHz and the beam width is 19° FWHM. The maximum radiated power from the antenna array is 1 MW, which is equivalent to 80 MW radiated isotropically at this fre-

quency. The calculated power density is 0.2 mW/m^2 with an oscillating *E*₀ field of 0.3 V/m at an altitude of 200 km before taking into consideration the enhancement of the *E* field as a result of plasma collective effects or absorption at lower heights (*D* and *E* regions). When directed vertically, the angular spread in the main beam covers a range of angles (6° to 32°) with respect to the Earth's magnetic field, which is inclined at an angle of 13° with respect to the vertical. The ray paths computed from a cold-plasma theory are plotted in Fig. 1 using an experimentally observed density profile deduced from an ionogram. The resonant interaction region at the height *h*, $\omega_0 = \omega_p(h)$, has an elliptical shape with its long axis pointing towards the magnetic north in the magnetic meridian plane; the rays stay parallel to the resonant layer, with their polarization vector, *E*, mainly along *B*₀ for a significant distance (30 km), a consequence of the long density gradient length. This ray trajectory is important in the explanation of the efficient coupling of the EM radiation with the polar ionosphere.

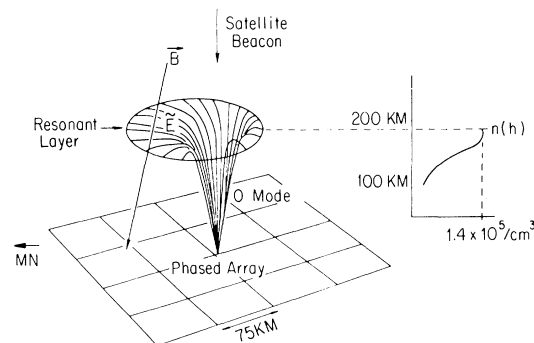


FIG. 1. Schematic showing the EM rays and their trajectories in the ionosphere where the Earth's magnetic field *B*₀ makes an angle of 13° with the density gradient. All the rays in the meridian plane within 7° of the vertical reach the resonant layer $\omega_0 = \omega_{p,\text{max}}$. The northward rays stay parallel to the resonant layer for 30 km.

The changes in the ionospheric density profile were systematically observed with an ionosonde. A series of short (30 μ s) EM pulses of frequency range 1.6 to 6 MHz was sent up to the ionosphere. A pulse whose spectrum centers about frequency ω is reflected at the height h , where $\omega = \omega_p(h)$. Since the total time required for the pulse to travel back to the ground receiver is $\tau = \int_0^h dh/v_g$, where v_g is the group velocity and h is the height for a given plasma frequency, the density and the height can be calculated from the elapsed time τ . The plot of τ versus the sounding frequency f is called an ionogram. When the sounding is performed in the O mode, the maximum frequency for which a return is obtained is the peak plasma frequency of the ionospheric density profile.

A sequence of ionograms was made with the SRI digital ionosonde after successive excitation by the heater. The sounder, when operating with one dipole antenna, has a large (90°) viewing angle of the ionosphere, and is sensitive mainly to large-scale perturbations. A receiving array of eight antennas, of the same size as the high-power transmitting array and located 400 m east of it, was used to detect both the amplitude and phase of a probing EM wave reflected from the resonant layer. A computer-generated skymap, constructed from a superposition of the radiation patterns of the receiving antennas, shows a horizontal extent (60 km) elongated towards the magnetic north. It is qualitatively similar to the illuminated region determined from the ray-tracing code as shown in Fig. 1.

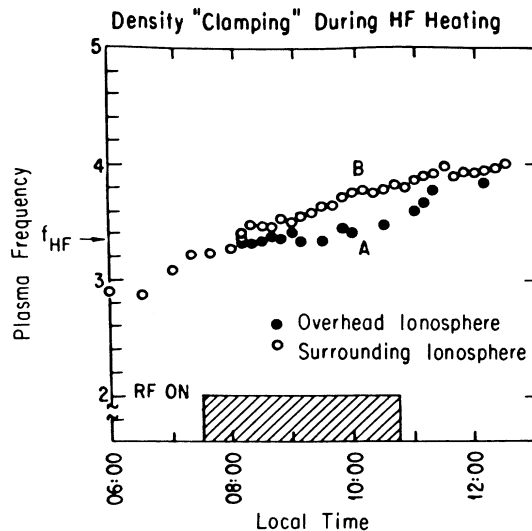


FIG. 2. Evolution of the ionospheric density in the heated region (trace A) and the unperturbed neighboring region (trace B) during the normal rise in the morning due to solar radiation. The heater was on during 2 May 1987, 0730–1045 Alaska local time (1530–1845 UT). Similar observations were made during 17 April, 0800–1000; 20 April, 0830–0930; 23 April, 0800–1000; and 4 May, 0830–0900 Alaska local time.

The most dramatic changes were observed during five morning runs, when the ionosphere normally increases as a result of solar radiation. When the high-power radiating facility (hereafter referred to as the heater) is turned on, the maximum ionospheric density in the overhead region was observed to be clamped at a plasma frequency equal to the excitation frequency. The ionogram recorded the density profiles from both the heated and nonheated regions. The heated region was clamped while the neighboring region continued to increase in density. As shown in Fig. 2, the densities in the two regions began to diverge within 20 min after the heater was turned on, and converged in approximately the same time, after the heater was turned off. By comparison with the normal increase of the ionospheric density, which has a measured value of $dn/dt \cong 10 \text{ cm}^{-3}/\text{sec}$, we deduce that the heater must have expelled particles out of the resonant region at the same rate in order to keep the density constant in the main heated region. The long recovery time of the perturbation is consistent with its large-scale size and implies a drift velocity to be less than 60 m/sec.

The HIPAS-induced ionospheric density perturbation may have caused changes in the phase shift of a satellite radio beacon passing over the heated region at an altitude of 1000 km. Analysis of these phase shifts at uhf (413 MHz) disclosed a sharp gradient in the total electron content³ (TEC), $\int n ds$, where s is along the line of sight between receiver and satellite, as shown in Fig. 3. A reduction in TEC by 30% was observed when the propagation vector of the satellite beacon traversed the

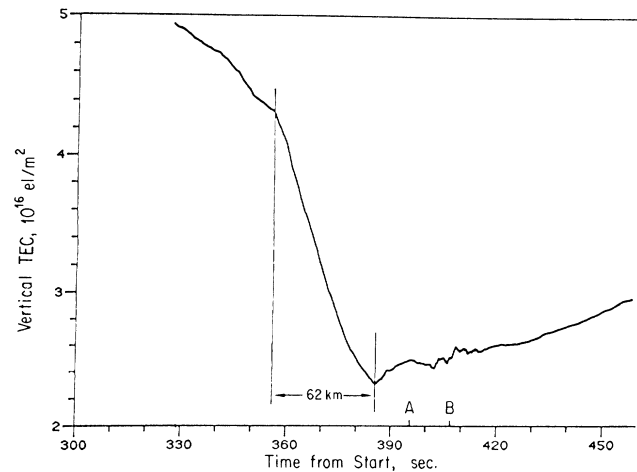


FIG. 3. Sharp gradient in the total electron content observed with the Polar Bear satellite which moved from north to south over HIPAS through a maximum elevation angle of 82°, at a height of 1000 km. At 395 sec after the beginning of the pass, the line of sight between the satellite and the receiving station scanned within 15 km of the center of the heated region (point A). A weak local maximum in intensity scintillation occurred near the magnetic zenith (point B). The observation was conducted in the early morning of 17 April 1987, 0737–0750 Alaska local time (1537–1550 UT).

heated region over HIPAS. The duration of the TEC depletion corresponds to a region of 60 km in horizontal extent at a height of 225 km, the height of the resonant layer derived from the ionogram. This horizontal extent is the same as the coverage of the hf antenna pattern. Coupling the change in the line integral of the density (TEC) with the plasma density profiles and the difference in densities between neighboring regions as deduced from the ionograms, we found that the perturbed region was 300 km in vertical extent. We note that similar but more gradual TEC gradients sometimes occur naturally in the morning hours near HIPAS. Enhanced phase and amplitude scintillations of the satellite beacons at uhf and vhf were also observed when the satellite traversed the region irradiated by HIPAS, indicating the presence of field-aligned density striations.² These satellite-beacon observations were conducted during the morning periods, when the optimum frequency-matching condition was satisfied.

The frequency-matching condition was also achieved during the evening when the ionospheric density was decreasing. As soon as the excitation frequency matched an ionospheric layer with a small density gradient, a large spread in the ionogram was observed in both the *X* and *O* traces (Fig. 4). This heater-induced spread in the ionosonde returns has been interpreted² as due to the generation of density irregularities aligned along the magnetic field.

The large-scale modification that results from exactly matching the excitation frequency with the ionospheric plasma frequency in the gentle gradient region can be explained by the propagation pattern of the EM rays and the efficient conversion of EM waves to electrostatic (ES) waves at the resonant layer. At this layer the *E* field becomes polarized along the nearly vertical ambient magnetic field^{4,5} and has a large component along the density gradient in this polar geometry. Calculations using a 3D cold-plasma ray-tracing code for the propagation of EM waves in the *O* mode show that all the EM waves within a cone of 7° from the vertical reach the resonant layer. The rays stay parallel to the plane of constant density for a total horizontal extent of 60 km. The gentle density gradient is responsible for fanning out the beam at the peak of the density profile and explains the extent of the horizontal perturbation.

A particle-in-cell computer simulation⁶ with three velocity and two spatial coordinates obeying the full set of Maxwell equations was used to investigate the coupling between EM and ES waves in the vicinity of the resonant region. This code follows the motion of particles in the presence of self-consistent time-varying *E* and *B* fields and allows a static magnetic field at an angle (10°) with respect to the density gradient. Effects of finite-temperature, density gradient, and magnetized behavior are included. The simulation results show how the initial circular polarization of *O* mode becomes elliptical as it approaches the resonant layer where electrostatic fields,

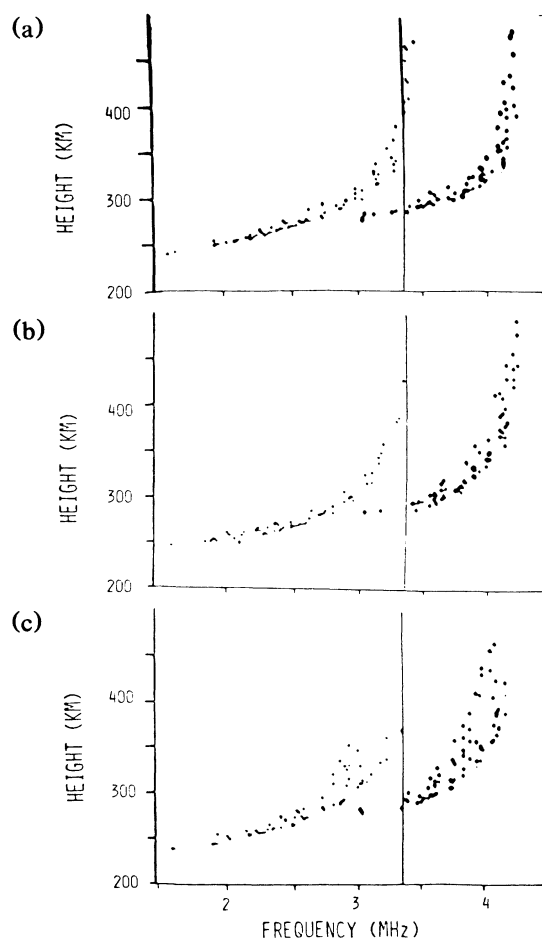


FIG. 4. Ionograms taken during evening (8 October 1986, 2030–2044 Alaska local time) when the excitation frequency is just below the peak ionospheric plasma frequency. The natural plasma production rate is negligible. (a) Ionogram taken at 2030, just before the heater is turned on. (b) Ionogram taken at 2035 after 4 min of heating at *O* mode. Radiated power is 0.525 MW. The frequency is 3.450 MHz. Note the reduced return at the resonant layer where the heating frequency is denoted by the vertical line. (c) Ionogram taken at 2044 after 2 min of heating at *O* mode. Note the enhanced spread returns in both the *O* and *X* traces. All ionograms were taken when the heater was off.

which are initially absent, develop to amplitudes much larger than the incident field. After 160 electron plasma periods, these ES fields become highly localized (Fig. 5) with a spatial scale length of approximately 0.1-EM wavelength (or 20-Debye lengths).

To follow the evolution of the small incident *E* field more accurately we made use of the fact that *E* is aligned along the density gradient at the resonant height and used a simplified 1D code with 225000 particles. The simulation showed that $E^2/4\pi nkT$ is enhanced by 4 orders of magnitude at the resonant layer from 10^{-4} to unity. In both simulations we have shown that mobile

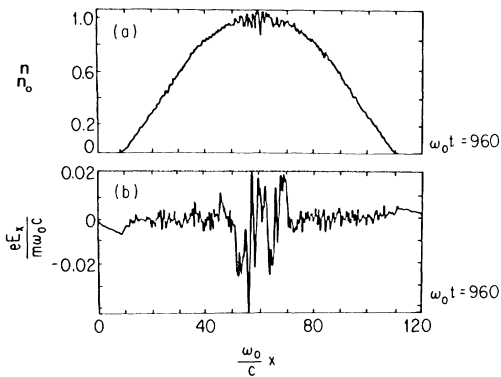


FIG. 5. Computer simulation of the evolution of the density profile subject to an O -mode EM wave whose frequency matches the plasma frequency at the flat top. The number of particles used in the simulation was 96 000 with a mass ratio of 1600 and the initial profile is inverse parabolic. (a) After 150 electron plasma periods, multiple spiky cavitons of roughly 10% depth with spatial size of $20\lambda_d$ have formed. (b) The external driving field E_0 is enhanced by a factor of 10 and the energy density, $|E^2|/4\pi nkT_e$, from 10^{-2} to 1.

ions are essential to provide highly localized intense electric fields.

A complementary laboratory experiment⁷ in argon plasma was used to verify the large enhancement of the fields at the resonant layer. The low-excitation field intensity, $W = E^2/4\pi nkT_e \cong 10^{-3}$, was enhanced to 10^{-1} and created a density cavity of 30% depression at the top of the density profile. The density cavity covers a region equal to the scale size of the density gradient and is many Debye lengths ($> 10^3$) across.

Analytic theory⁸ has predicted the conversion from EM to ES waves through the modulation instability in a uniform quiescent plasma. The threshold of this instability, in the absence of convection, is $E^2/4\pi nkT \sim 8\nu/\omega_p \sim 10^{-4}$, where ν is the electron-neutral collision frequency at 200 km. The field strength of the EM wave radiated by HIPAS ($E^2/4\pi nkT = 6 \times 10^{-4}$) exceeds this threshold.⁹ According to the caviton model¹⁰ the oscillating electric field and density cavity evolve and enhance one another because of the trapping of the wave field by density cavities.

In the HIPAS experiment density clamping occurred during the morning periods when the particles expelled by the caviton fields along the magnetic field and the new particles created by the solar radiation balance each other. The resonance matching is therefore sustained over a long period of time and over a large spatial extent. The density of the neighboring region, which is not being irradiated by the EM wave, rises normally as a result of the ionization by solar radiation. A density trough elongated along the magnetic field is then created, which can account for the sharp gradient in the total electron content between the heated and the nonheated regions, as observed by using the satellite beacon.

In summary, our field experiment demonstrates an optimal condition of effecting large-scale changes in the polar ionosphere by remote ground-based rf transmitters. Computer and laboratory modeling proposed a plausible process for the creation of a large-scale density depression out of the small-scale acceleration by many localized cavitons. However, individual cavitons were not resolved by the diagnostics in the present experiment. This paper does not attempt to resolve the competition between cavitons and striation phenomena or offer an unequivocal explanation of the TEC data. These must be determined by *in situ* diagnostics on board of future rocket flights or satellites with low-perigee orbits.

We acknowledge the assistance of J. Carroll, W. Huhn, R. Dickman, W. Harrison, B. Lum, and G. Wong of HIPAS, A. McKinley of SRI, Professor R. Hunsucker of the University of Alaska, J. Lansinger of Northwest Research Associates (NwRA), Dr. D. DuBois of LANL, and Dr. V. Decyk of University of California, Los Angeles (UCLA). Research at HIPAS was supported by ONR, the participation of NwRA supported by the Defense Nuclear Agency, and research at LLNL supported by DOE.

¹A. V. Gurevich, in *Nonlinear Phenomena in the Ionosphere*, edited by L. J. Lanzerotti and D. Stöfler, Physics and Chemistry in Space Vol. 10 (Springer-Verlag, New York, 1978).

²E. M. Allen, G. D. Thome, and P. B. Rao, *Radio Sci.* **9**, 905 (1974); P. Stubbe, H. Kopka, H. Lauche, M. T. Rieveld, A. Biecke, O. Holt, T. B. Jones, T. Robinson, A. Hedberg, B. Thide, M. Crockett, and H. J. Lotz, *J. Atmos. Terr. Phys.* **44**, 1025 (1982); A. Y. Wong, J. Santoru, C. Darrow, L. Wang, and J. Roederer, *Radio Sci.* **18**, 815–830 (1983); W. Birkmayer, T. Hagfors, and W. Kofman, *Phys. Rev. Lett.* **57**, 1008 (1986); A. Y. Wong, T. Tanikawa, and A. Kuthi, *Phys. Rev. Lett.* **58**, 1375 (1987); L. M. Duncan, J. P. Sheerin, and R. A. Behnke, *Phys. Rev. Lett.* **61**, 239 (1988).

³A. A. Burns and E. Fremouw, *IEEE Trans. Antennas Propag.* **18**, 785 (1970).

⁴V. L. Ginzburg, *The Propagation of Electromagnetic Waves in Plasmas* (Pergamon, Oxford, 1970).

⁵K. G. Budden, *The Propagation of Radio Waves* (Cambridge Univ. Press, London, 1985), p. 274; E. Mjølhus and T. Fla, *J. Geophys. Res.* **89**, 3921 (1984).

⁶C. K. Birdsall and A. B. Langdon, *Plasma Physics via Computer Simulation* (McGraw-Hill, New York, 1985).

⁷B. S. Bauer, L. Scurry, and A. Y. Wong, *Bull. Am. Phys. Soc.* **9**, 1752 (1987).

⁸K. Nishikawa, *J. Phys. Soc. Jpn.* **24**, 1152 (1968).

⁹If initial density perturbations are present in the ionosphere the conversion can proceed by the process of direct mode conversion for which there is no threshold; A. Y. Wong *et al.* *Phys. Rev. Lett.* **47**, 1340 (1981); D. Dubois, D. Russell, and H. Rose (private communication).

¹⁰V. E. Zakharov, *Zh. Eksp. Teor. Fiz.* **62**, 1745 (1972) [*Sov. Phys. JETP* **35**, 908 (1972)]; H. C. Kim, R. L. Stenzel, and A. Y. Wong, *Phys. Rev. Lett.* **33**, 886 (1974); G. J. Morales and Y. C. Lee, *Phys. Rev. Lett.* **33**, 1534 (1974); T. Tanikawa, A. Y. Wong, and D. L. Eggleston, *Phys. Fluids* **27**, 1416 (1984).